THE ASTROPHYSICAL JOURNAL, 206:138–149, 1976 May 15

EVOLUTION OF ROTATING INTERSTELLAR CLOUDS. II. THE COLLAPSE OF PROTOSTARS OF 1, 2, AND 5 $M_\odot$

DAVID C. BLACK
Space Science Division, NASA-Ames Research Center
AND
PETER BODENHEIMER
Lick Observatory, Board of Studies in Astronomy and Astrophysics, University of California, Santa Cruz; and Space Science Division, NASA-Ames Research Center
Received 1975 July 16; revised 1975 October 27

ABSTRACT

Numerical calculations have been made for the early stages of collapse of axisymmetric, rotating protostars of 1, 2, and 5 $M_\odot$. The calculations employ a range of values of total angular momentum, as well as two types of initial density distribution. The effects of boundary conditions are tested by using constant volume and constant surface pressure with identical initial conditions. The principal result of the calculations is that in all cases tried the collapse leads to the formation of a ring structure in the interior of the cloud, with a local density minimum at the center of the cloud. The rings approach equilibrium with a structure consistent with that of previous analytic determinations (Ostriker), after which they undergo further gravitational collapse. The collapse of a 2 $M_\odot$ cloud, similar to that assumed by Cameron and Pine, does not appear to lead to the equilibrium nebula these authors construct.

Subject headings: nebulae: general — stars: formation

I. INTRODUCTION

It has long been recognized that angular momentum is an important, indeed crucial, quantity that must be considered in a theory of star formation; however, detailed numerical calculations with its inclusion have been few in number. Lin, Mestel, and Shu (1965) undertook an analytic calculation of the collapse of a rotating, pressure-free spheroid. Hara, Matsuda, and Nakazawa (1973) have calculated cloud collapse, including the effects of pressure and rotation, under the assumptions that the cloud contracts isothermally and that all equidensity surfaces retain spheroidal shapes. Larson (1972) has made a full numerical calculation of the collapse of axisymmetric rotating clouds, including effects of pressure and radiative transfer and without any restrictive hypothesis on the shape of equidensity surfaces. Larson's numerical grid contained approximately 72 cells. An important feature of his results is the development of a ringlike structure in the inner parts of the cloud, with a local density minimum at the center of the cloud. However, Tscharnuter (1975) considered the same problem using different numerical techniques and did not find rings. Two-dimensional calculations of gravitational collapse have also been carried out by LeBlanc and Wilson (1970), including the effects of rotation, magnetic fields, and neutrino transport. The problem they treated concerned the late stages of evolution of a massive star, with collapse induced by thermal decomposition of iron.

In this paper we present detailed calculations of the evolution of rotating protostars which are assumed to start out as gravitationally bound configurations with radii slightly less than the Jeans radius. The physical assumptions are comparable with those of Larson. Physical processes leading to transport of angular momentum, such as viscosity, are not included in the equations. The grid contains 1600 cells, and the calculations are performed with the two-dimensional hydrodynamic code (with the assumed axial symmetry) discussed by Black and Bodenheimer (1975, hereinafter Paper I). We consider the following questions:

1. How does the behavior of the collapse depend on total mass and angular momentum?
2. How do the results depend on the assumed initial and boundary conditions?
3. Is the occurrence of ring formation, first noted by Larson (1972), confirmed?
4. Do nonaxisymmetric instabilities occur in collapsing rotating clouds, and do binary systems form as a result?
5. Is the model "solar nebula" calculated by Cameron and Pine (1973) consistent with the results of hydrodynamic calculations?

The physical equations and the parameters for the evolutionary runs are discussed in § II. The results are presented in § III. In § IV we discuss the results and summarize the progress that has been made in the resolution of the five questions posed above.

II. CALCULATIONS

The physical equations and numerical method of solution are discussed in detail in Paper I. We use cylindrical coordinates R, θ, and Z and express the

equations with respect to a moving Eulerian grid. We include the standard hydrodynamic equations of continuity, momentum, and energy, and obtain the gravitational field by finding the steady-state solution of a diffusion equation closely related to Poisson's equation (Peaceman and Rachford 1955; Paper I, § III*f*). Boundary values for the gravitational potential are calculated from the first three nonzero moments of the mass distribution. Radiative transfer is treated by a standard diffusion approximation, with material temperature assumed equal to radiation temperature. The solution is obtained by means of an alternating-direction implicit technique described in § III*c* of Paper I. The radiative opacity for the calculations discussed here is due primarily to dust grains; we approximate the Rosseland mean opacity by the constant value $\kappa_R = 0.15$ cm^2 g^{-1} for all temperatures less than 1400 K. The equation of state is discussed in § II of Paper I. The present calculations terminate at rather low temperatures, before effects of dissociation, ionization, or radiation pressure become important. In order to obtain a reasonable comparison with the work of Larson, we have adopted for the purposes of this paper the simplified equation of state for molecular hydrogen that he used, with specific internal energy given by $E(H_2) = 5R_gT/(2\mu)$, where R_g is the gas constant and the mean molecular weight $\mu = 2$.

All calculations start with a spherical, uniformly rotating, gravitationally bound configuration of pure molecular hydrogen at an assumed uniform temperature of $T = 10$ K. The initial density is taken to be uniform over the sphere except in the special case (2B) mentioned below, and fluid velocities U and W in the R- and Z-directions, respectively, are taken to be zero. A particular evolutionary calculation is specified by the following parameters: the total mass M; the ratio α of the initial total radius R_* to the Jeans length $R_J = 0.42GM\mu/(R_gT)$; and the initial ratio, β, of the total kinetic energy of rotation to the absolute value of the gravitational potential energy. In the presence of rotation the Jeans criterion is modified to become (Larson 1972)

$$R_* \leq \frac{0.42GM}{R_gT/\mu + E_R}, \tag{1}$$

for the case of a uniformly rotating configuration of uniform density, where E_R is the rotational energy per unit mass of the configuration. If M and β are specified, relation (1) leads to the following condition on α if collapse is to occur:

$$\alpha \leq 1 - 1.43\beta. \tag{2}$$

In practice, α was set to 0.52 for all runs reported here; this is sufficiently small to allow collapse for all values of β up to 0.34. The total angular momentum (cgs) in terms of the specified parameters is

$$J = 1.3 \times 10^{55}\left(\frac{M}{M_\odot}\right)^2\left(\frac{\alpha\beta\mu}{T}\right)^{1/2}, \tag{3}$$

for the case of a uniform sphere in uniform rotation. As indicated in Paper I, J is conserved in all calculations.

The initial parameters, properties, and assumed boundary conditions of the seven runs to be discussed here are summarized in Table 1. Angular momentum J, initial angular velocity ω_0, and initial density ρ are given in cgs units. Case 2B was calculated with a centrally concentrated initial density distribution given by $\rho(r) = \rho(0)(1 - r/R_*)$, where r is the distance to the center and R_* is the total radius. All cases were calculated with a constant pressure (equal to the initial pressure) on the outer boundary, with the exception of case 1D in which the volume of the protostar was fixed at its initial value. The constant volume condition was employed by Larson (1972).

The closest direct comparison with the calculation described in detail by Larson is provided by case 1D, which employs a comparable boundary condition but differs somewhat in other parameters. His calculation also starts with a uniform density and uniformly rotating configuration at $T = 10$ K, and with fluid velocities equal to zero. The rotational energy and initial radius of Larson's model correspond to values of 0.22 and 0.59, respectively for β and α. His cloud has $M = 1\ M_\odot$ with initial density of 4.77×10^{-19} g cm^{-3}. A slight compositional difference exists between Larson's models and ours in that his have $\mu \approx 2.5$. A comparison with the equilibrium model of the solar nebula calculated by Cameron and Pine (1973) is provided by case 2B, which employs the same total mass, total angular momentum, and initial distributions of density and angular velocity as they assumed. Again, there are small differences in composition.

TABLE 1

INITIAL CONDITIONS

Case	$M/M_\odot$	β	J (g cm^2 s^{-1})	ω_0 (rad s^{-1})	ρ (g cm^{-3})	B.C.
1A.....	1	0.02	6.0(53)	1.52(−13)	1.38(−18)	const. pressure
1B.....	1	0.08	1.2(54)	3.04(−13)	1.38(−18)	const. pressure
1C.....	1	0.32	2.4(54)	6.08(−13)	1.38(−18)	const. pressure
1D.....	1	0.32	2.4(54)	6.08(−13)	1.38(−18)	const. volume
2A.....	2	0.08	4.8(54)	1.52(−13)	3.45(−19)	const. pressure
2B.....	2	0.0025	8.2(53)	3.14(−14)	9.96(−19)*	const. pressure
5A.....	5	0.08	3.0(55)	6.08(−14)	5.52(−20)	const. pressure

* Central density.

III. RESULTS

It was found that the seven cases calculated during this work exhibited qualitatively similar behavior, but differed in quantitative detail. Consequently, the first part of this section is devoted to discussion of the principal qualitative features of the collapse, while the latter part concerns the differences between the individual cases.

a) General Characteristics of the Collapse

There are five general phases in the evolution: (1) an initial phase, comparable in duration with the free-fall time, during which the cloud loses spherical symmetry and becomes highly flattened; (2) the formation of an axisymmetric, ringlike structure in the inner part of the cloud; (3) a phase during which the ring approaches equilibrium; (4) a collapse of the ring upon itself; and (5) the ejection of a high velocity "sheet" of material from the outer periphery of the ring. The total time scale for the last four phases is in general shorter than that of the first phase; the last three phases occur over a very short time scale compared with the total evolutionary time.

i) *Phase I: Flattening*

During the initial phase of the collapse, motion of the fluid in the Z-direction (parallel to the rotation axis) is similar to that obtained in calculations of the collapse of nonrotating clouds. Pressure gradients have a significant effect in slowing down the collapse. However, since motion of the fluid in the R-direction is additionally retarded by the effects of rotation, an asymmetry in the density distribution develops. The density distribution becomes centrally condensed and the evolutionary time scale becomes much shorter in the central regions that in the outer regions. After the collapse has proceeded approximately one free-fall time, the effects of rotation are well marked. The low angular momentum material near the rotation axis collapses toward the equatorial plane, producing a highly flattened structure. On the same time scale, however, the lower density material away from the axis has not had a chance to collapse to the plane and retains a more nearly spherical distribution. The overall structure at the end of this phase is a toroidal configuration, highly flattened at the pole. A relatively small volume approximating a uniform-density, oblate spheroid remains at the center (case 2B excepted). The rotational energy of this central region is small compared with both its internal and gravitational energies. The optical depth of the cloud during this phase is low enough to permit the full escape of compressional heat, and the cloud remains isothermal.

ii) *Phase II: Ring Formation*

By the end of Phase I, the inner portions of the cloud evolve on a much shorter time scale than does the cloud as a whole. The central, highly flattened region of the cloud continues to increase in mass. After the density in the inner region has increased by a factor of ~ 10–100 over its value at the end of Phase I, a density maximum begins to form in the previously uniform central regions of the cloud. The point of maximum density lies in the equatorial plane and away from the rotation axis; that is, a ringlike structure begins to form in the interior of the cloud. After the ring has started forming, the R-component of velocity of material interior to the ring changes sign, and this material begins to flow slowly outward toward the minimum in gravitational potential which is now located at the center of the ring. As a consequence of this outward flow of material, the central density begins to decrease, and a sharp density contrast develops between the ring and the center of the cloud (a factor of ~ 500 in some cases). It is important to note that in all cases, ring formation begins *prior* to large-scale flow outward from the center of the cloud. Also, the existence of a uniform-density region is *not* necessary for ring formation to occur (see below). Once formed, the ring continues to gain mass at an increasing rate, while its distance from the rotation axis increases somewhat and then becomes well fixed. Experiments with different zoning and spatial resolution in the numerical grid, as well as with different boundary conditions, lead us to conclude that the reality of the rings is well established. In all cases, except 2B, the ring begins to form while the material is optically thin and isothermal at $T = 10$ K.

iii) *Phase III: Ring Equilibrium*

The formation and subsequent growth of the ring in Phase II is wholly dynamic. However, as the ring continues to grow by accretion of surrounding material, the translational energy (R and Z motion) of material *in* the ring decreases, and the ring approaches equilibrium. Additional evidence that the ring is near equilibrium is afforded by a detailed examination of the contributions to the momentum equation. Results from case 1D show that the quantity

$$\delta \equiv \sum_i F_i / \sum_i |F_i| ,$$

where the F_i represent the pressure, gravitational, and rotational contributions to the inertial equation, is typically $\lesssim 0.05$ throughout the ring. A comparison with the analytic results of Ostriker (1964) will be made later in the paper. Phase III is also characterized by the formation of a roughly spherical shock front whose strength varies with polar angle, being strongest at the pole and rather weak at the equator. The "radius" of this shock front is comparable with the distance from the rotation axis to the outer edge of the ring. Properties of the rings, calculated at times when they are well developed but not necessarily at the point of closest approach to equilibrium, are given in Table 2. The quantities ρ_c and $\rho_{\max}$ are, respectively, the central and the maximum ring densities. The distance from the rotation axis to the center of the ring is denoted by d.

TABLE 2

RING PROPERTIES

Case	β	Time (yr)	d (cm)	ρ_c (g cm^{-3})	ρ_{max} (g cm^{-3})	M_{ring}/M_{total}	t_{ff} (yr)*	M_{ring}/M_{total} (equilibrium)
1A.....	0.02	6.22(4)	3.4(14)	6.0(−15)	1.5(−12)	0.03	5.68(4)	0.03
1B.....	0.08	7.78(4)	2.6(15)	2.0(−16)	1.8(−14)	0.22	5.68(4)	0.10
1C.....	0.32	9.52(4)	5.7(15)	1.3(−16)	8.7(−15)	0.32	5.68(4)	0.22
1D.....	0.32	1.46(5)	6.0(15)	9.9(−17)	1.7(−15)	0.22	5.68(4)	0.23
2A.....	0.08	1.56(5)	4.8(15)	5.8(−17)	3.8(−15)	0.16	1.13(5)	0.09
2B.....	0.0025	1.00(5)	9.0(13)	1.0(−13)	2.3(−11)	†	6.68(4)	†
5A.....	0.08	3.62(5)	1.3(16)	4.3(−18)	3.2(−16)	0.11	2.84(5)	0.10

* Free-fall time.

† Ring mass not calculated.

iv) *Phase IV: Ring Collapse*

As noted above, Phase III, which typically lasts about 10 time steps, is characterized by relatively detailed force balance (small δ) throughout the ring. Gravitational forces then begin to dominate over both pressure and rotational effects as the result of a strong, approximately symmetric, steepening of the potential well about the ring center. During this phase, the mass and angular momentum contained in the ring region increase rapidly. The δ-values for case 1D are uniformly $\lesssim 0.05$ during Phase III, but a short time later the δ-value at the ring center increases to 0.42. The time scale for development of this collapse is in all cases consistent with the dynamic time scale of the ring itself. At approximately the same time, the distribution of specific angular momentum immediately outside the ring becomes unstable in the R-direction (cf. Goldreich and Schubert 1967); that is, it develops a local minimum with respect to the ring. Transport of material outward should result, on a time scale which according to Kippenhahn (1969) is greater than or equal to the Kelvin time; this transport was not included in the calculation.

Evolution of the ring up to and through Phase IV systematically produces progressively stronger gradients of quantities in the ring volume. At the end of Phase IV, variations in density and angular momentum between adjacent zones in the ring have become large enough so that numerical results are certainly not quantitatively correct, and only future work will demonstrate whether the behavior identified as Phase V is qualitatively correct. This caveat should be borne in mind in relation to Phase V.

v) *Phase V: "Sheet" Ejection*

This phase is characterized by three distinct events: a rapid buildup of rotational energy in the ring, ejection of mass and angular momentum from the ring, and inward motion of the ring. The buildup of rotational energy occurs over a very short time scale and begins with the later stages of Phase IV. During this buildup, integral checks on energy conservation show that energy does not appear to be conserved, possibly as a result of inaccuracies in the checks themselves. Immediately following the increase in the rotational energy of the ring (all other energies associated with the ring, as well as its mass, are also rapidly increasing at this point), material at the outer periphery of the ring is ejected from the ring and moves outward, approximately normal to the rotation axis, at a high velocity ($\approx$1–20 km s^{-1}). The outward flow is confined to a region only a few zones thick (in Z); hence the identification as a "sheet." The vertical thickness of the sheet corresponds closely to the Z-extent of the ring. The amount of mass ejected is difficult to determine, but it may be as much as 10 percent of the ring mass in the more rapidly rotating cases. The ejected material has a relatively high specific angular momentum. Certain calculations were continued beyond the point of sheet ejection; they indicate that the ring subsequently moves closer to the rotation axis. Although energy does not appear to be conserved during the rapid buildup of rotational energy, it is conserved quite well once ejection starts. The excess rotational energy in the ring appears directly in the kinetic energy of the ejected sheet. In several of the cases, the kinetic energy gained by the sheet appears to be sufficient to allow some of the sheet material to escape from the cloud.

b) Comparison of Individual Cases

Cases 1A, 1B, and 1C represent a sequence with increasing β but with otherwise identical properties. All calculations were carried out for somewhat longer than one free-fall time. As β is increased, the evolution time increases, as rotation is more effective in slowing down the collapse in its early stages. Also, with an increase in β, the ring forms at a greater distance from the rotation axis and has a larger fraction of the total mass and a lower mean density. Escape velocity is attained in the sheet ejection process in cases 1B and 1C, but not in 1A. The configurations remain isothermal throughout the evolution in cases 1B and 1C, but the densities attained in case 1A are high enough so that a small amount of heating takes place in the center; at the time of ring equilibrium the maximum temperature occurs in the ring and has a value of 24 K. The density, R-component of velocity, angular velocity, and specific angular momentum, as a function of distance from the spin axis and in the equatorial plane for case 1A, are shown at various evolutionary times in Figure 1. Note that the ring radius increases

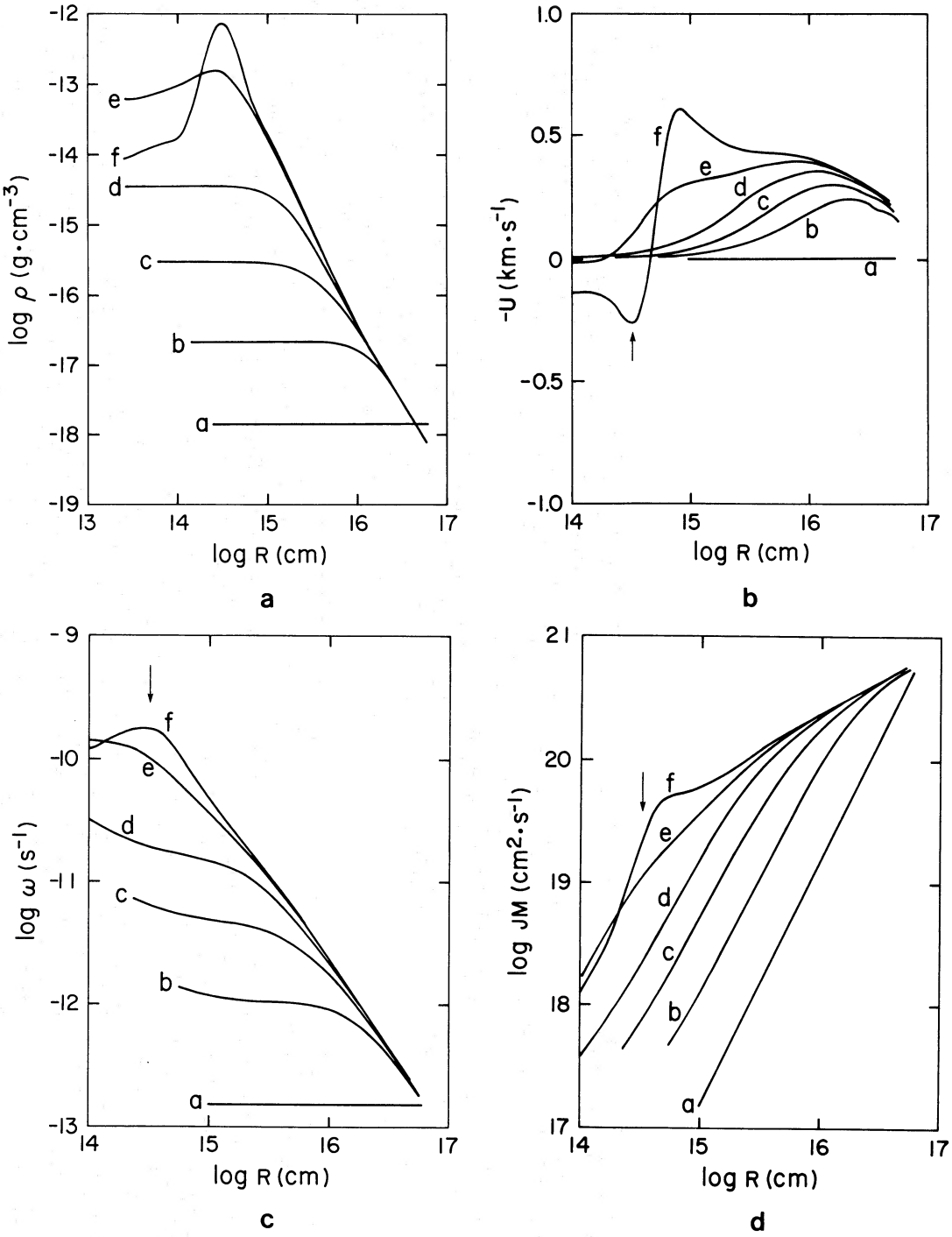

FIG. 1.—(*a*) Density, in the equatorial plane, as a function of distance from the rotation axis for case 1A. (*b*) *R*-component of velocity, in the equatorial plane, as a function of distance from the rotation axis for case 1A. (*c*) Angular velocity, in the equatorial plane, as a function of distance from the rotation axis for case 1A. (*d*) Specific angular momentum *JM*, in the equatorial plane, as a function of distance from the rotation axis for case 1A. The curves a, b, c, d, e, and f in Figs. 1*a*, 1*b*, 1*c*, and 1*d* correspond to the following evolutionary times, respectively: 0, 5.05, 5.71, 6.00, 6.14, and 6.19 in units of 10^4 years.

slightly as the ring increases in mass and that the ring is already defined before the central density begins to decrease. Note also that ω is fairly uniform in the central region of the cloud, and does not develop a local maximum until the ring is well formed. The specific angular momentum monotonically increases outward at all times represented in Figure 1. We discuss these points later in connection with possible nonaxisymmetric behavior. Density contours and associated velocity plots are shown for case 1B in Figures 2 and 3 for two different times—at the point where the ring is just beginning to form, and when the ring has become fully developed. Entries in Table 2 for cases 1B and 1C, and Figure 3, represent post-equilibrium configurations, while the entry for case 1A represents a point very close to equilibrium.

Cases 1B, 2A, and 5A represent a sequence with β fixed at 0.08 and with increasing mass. The ratio of evolution time at the point of ring formation to free-fall time is the same in all cases. The ring radii are approximately proportional to the initial cloud mass. The detailed structure of the ring varies somewhat as a function of total mass with the low mass rings being more sharply peaked than the high mass rings. The fraction of *total* cloud mass contained in the ring, when it is close to equilibrium is practically independent of total mass. The entries in Table 2 do not reflect this fact, since that for case 5A represents a time close to equilibrium, while those for cases 2A and 1B represent rings which have evolved progressively farther beyond equilibrium and have rapidly increased their masses. In the last column of Table 2 we give estimated values for the equilibrium ring masses for those rings that are not in equilibrium.

Case 2B represents a collapse starting from an initial model closely corresponding to that assumed by Cameron and Pine (1973) in their construction of an equilibrium model of the solar nebula. Our initial

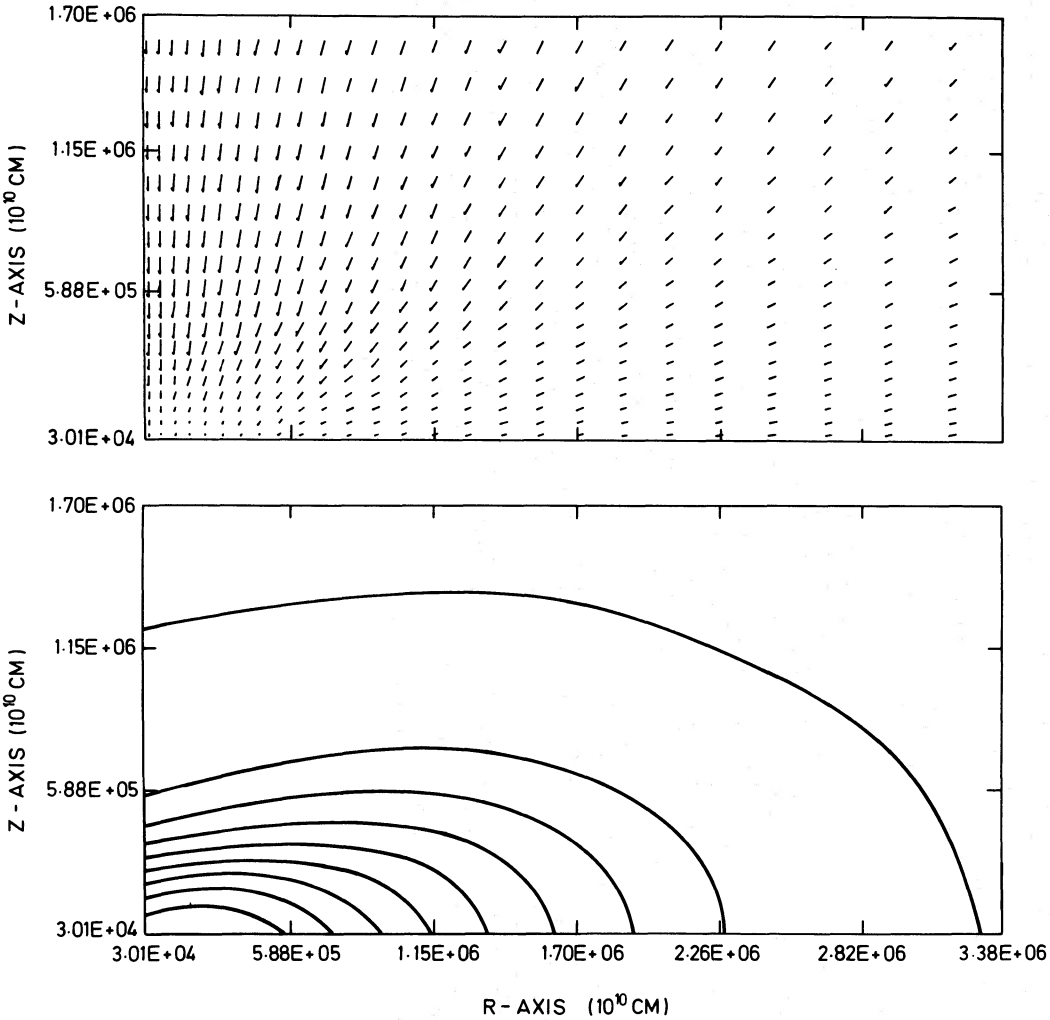

FIG. 2.—Detailed characteristics of the inner regions of case 1B at 6.83×10^4 years. *Upper*, velocity vectors with length proportional to speed. Maximum vector length corresponds to 0.52 km s^{-1}. *Lower*, equidensity contours corresponding to $\rho = \alpha^n \rho_0$, where $\rho_0 = 2.08 \times 10^{-16}$ g cm^{-3} and $\alpha = 0.645$ for $n = 0, 1, \ldots, 7$. The outermost contour corresponds to $\rho = 4.00 \times 10^{-18}$ g cm^{-3}.

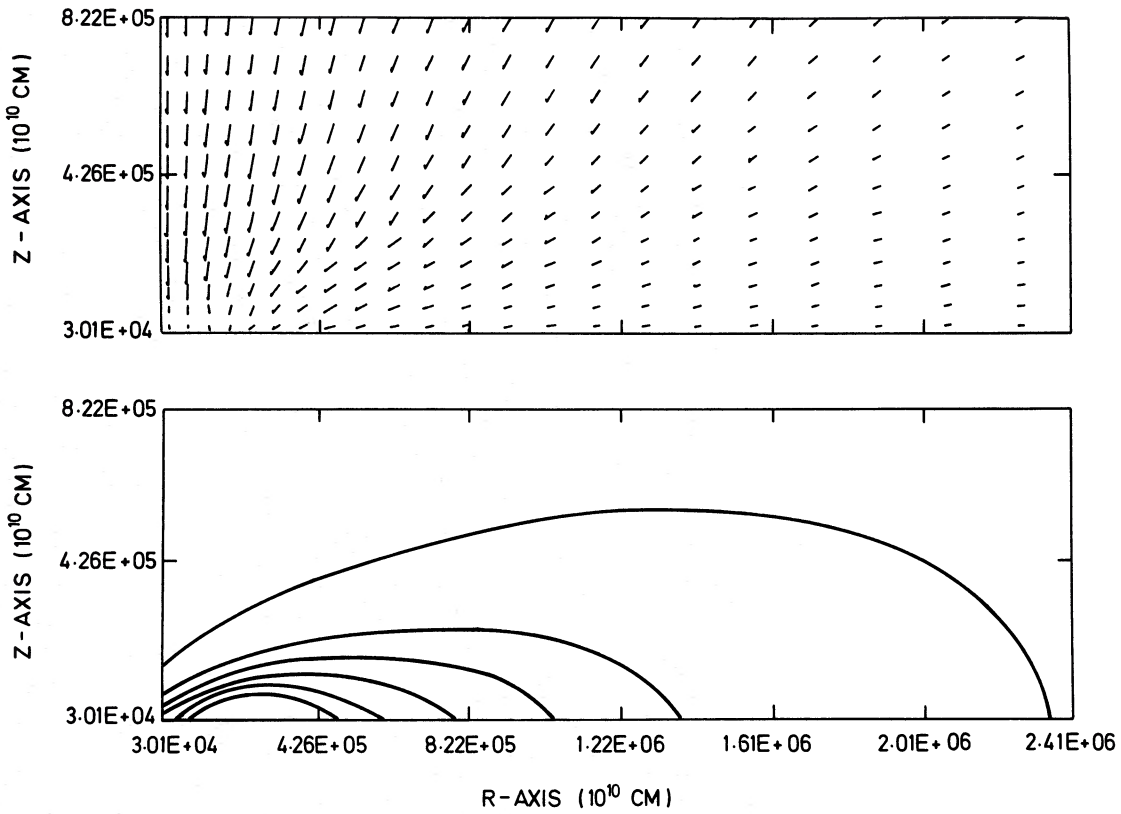

FIG. 3.—Detailed characteristics at the inner regions of Case 1B at 7.78×10^4 years. *Upper*, velocity vectors with length proportional to speed. Maximum vector length corresponds to 1.17 km s^{-1}. *Lower*, equidensity contours corresponding to $\rho = \alpha^n \rho_0$, where $\rho_0 = 7.10 \times 10^{-15}$ g cm^{-3} and $\alpha = 0.482$ for $n = 0, 1, \ldots, 7$. The outermost contour corresponds to $\rho = 1.00 \times 10^{-17}$ g cm^{-3}.

density distribution approximates their "linear sphere," a model in which density decreases linearly with distance from the center. The results are qualitatively similar to those of the other cases discussed here. Despite the low value of β ($\sim 2 \times 10^{-3}$) and the linear rather than uniform density distribution, ring formation proceeds in the usual manner. The ring radius of 9×10^{13} cm is smaller, and the density higher, than in the other cases. Consequently, some heating takes place in a very small mass fraction in the central regions. The density distribution near the end of the calculation does not resemble that in the Cameron-Pine model. In fact, the region interior to 1 AU contains very little material and has low temperature compared with that at the center of their nebula.

The effect on the collapse of using different boundary conditions is demonstrated by cases 1C (constant surface pressure) and 1D (constant volume). The process of ring formation and the resulting mass and radius of the ring are virtually identical in the two cases. The differences in ring properties listed in Table 2 are due to the fact that the ring in case 1C has evolved beyond the equilibrium point, while that for case 1D is close to equilibrium. The evolutionary time scale for case 1D was somewhat longer, and the distribution of material and the fluid velocities in the outer regions did differ in the two cases. The ring radius for case 1D is consistent with the results of Larson (1972); his value of 5×10^{15} cm is intermediate between the values we obtain for $\beta = 0.32$ and $\beta = 0.08$, consistent with his assumption of $\beta = 0.22$. Figure 4 illustrates the equilibrium ring properties for case 1D. We conclude that ring formation and evolution of the inner regions is relatively insensitive to the change in surface boundary conditions.

A rather narrow range of initial conditions is represented in the work reported here. All the configurations were initially uniformly rotating, so that the dependence of the results on the assumed initial rotation law is unknown. All calculations assumed that the fluid was initially at rest. We have made calculations of the collapse of a nonrotating cloud, employing the zero velocity initial condition, and have compared the results with those of a parallel calculation in which the fluid was assumed to be initially flowing inward in free fall. The general features of collapse were identical in the two calculations, differing only in time scale and minor quantitative features. However, the effect of free-fall initial conditions should be explicitly determined for the collapse of rotating clouds. The effect of the initial density distribution on the collapse is also unclear. Case 2B was run with an initial density distribution which decreased

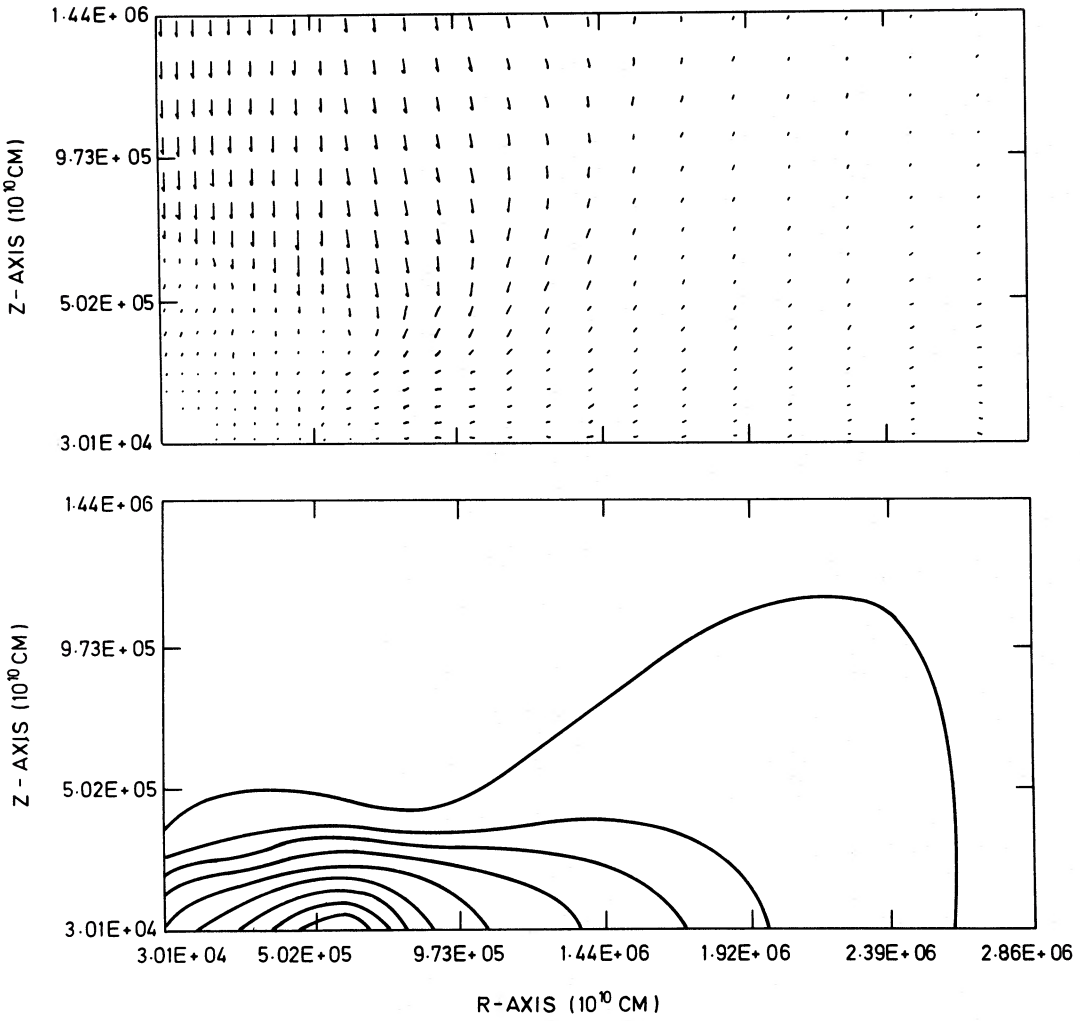

FIG. 4.—Detailed characteristics of the inner regions of case 1D at 1.46×10^5 years. *Upper*, velocity vectors with length proportional to speed. Maximum vector length corresponds to 0.90 km s^{-1}. *Lower*, equidensity contours corresponding to $\rho = \alpha^n \rho_0$, where $\rho_0 = 9.58 \times 10^{-16}$ g cm^{-3} and $\alpha = 0.551$ for $n = 0, 1, \ldots, 7$. The outermost contour corresponds to $\rho = 4.50 \times 10^{-18}$ g cm^{-3}. The fraction of total cloud mass contained within the outermost contour is 0.44.

linearly from center to surface, while all other cases were initially uniform in density. The conditions of case 2B are not directly comparable with any of the other cases, so we have not isolated the effect of the initial density distribution. Future experiments will address this point. It is clear, however, that ring formation occurs even when the initial density distribution is not uniform.

IV. DISCUSSION

For the purpose of the ensuing discussion, it is convenient to consolidate the five specific phases in the collapse (see § III*a*) into three broader categories—namely, (*a*) ring formation, (*b*) ring equilibrium, and (*c*) postequilibrium ring evolution. We discuss each of these in turn, and conclude with a discussion of other questions concerning the evolution of the entire cloud.

a) *Ring Formation*

It is tempting to attribute the formation of rings to one of the many instabilities associated with rotating, self-gravitating systems. The analysis of these instabilities is quite difficult, and most efforts to date have concentrated on equilibrium systems. In particular, analysis (cf. Bardeen 1971) of the sequence of Maclaurin spheroids (uniformly rotating, uniform-density configurations in hydrostatic equilibrium) shows that as the ratio β is increased, these configurations become secularly unstable to nonaxisymmetric perturbations ($\beta = 0.137$), dynamically unstable to nonasymmetric perturbations ($\beta = 0.274$), secularly unstable to axisymmetric perturbations ($\beta = 0.36$), and dynamically unstable to axisymmetric perturbations ($\beta = 0.46$). Ostriker and Bodenheimer (1973) showed that sequences of differentially rotating polytropes exhibit

secular and dynamic instability to nonaxisymmetric perturbations at about the same β values as the Maclaurin sequence. It is generally supposed that the instability at $\beta = 0.274$ leads to fission, and that the instability at $\beta = 0.46$ results in the formation of a ring.

There are, however, difficulties in applying existing analyses to the situation pertaining here. The formation of rings during the collapse is a wholly dynamic process, and it has not been shown that the equilibrium analyses may be generalized to nonequilibrium configurations. Also, these stability analyses refer to integral properties of the entire cloud, whereas ring formation involves only a portion of the cloud.

We can examine, nevertheless, whether the epoch of ring formation is associated with instability characteristics. It is likely that high local values of β and/or a critical degree of flattening are necessary, but not sufficient conditions for instabilities to arise. It was pointed out in § III*a* that the early phase of collapse leads to the formation of a highly flattened, disklike structure in the center of the cloud. The ring eventually forms in this region. However, the values of β in these disks are small, typically less than 0.1, indicating that ring formation is not characterized by locally high values of β. The ratio of polar to equatorial radii, a_3/a_1, of the disklike region may be used as an indicator of flattening. The first axisymmetric dynamical instability of Newtonian Maclaurin spheroids occurs when $a_3/a_1 = 0.04652$. However, the a_3/a_1 ratios in cases 1B and 1D at the time of ring formation were 0.237 and 0.325, respectively, much larger than that required for the dynamical ring instability. It would appear that ring formation is not a manifestation of a classic ring instability. Also, the fact that the a_3/a_1 ratio at the onset of ring formation is not the same in cases 1B and 1D suggests that ring formation does not depend on a critical a_3/a_1 value in the inner regions of the cloud.

The question arises as to whether ring formation is a result of a gravitational instability. The mass of the inner regions in which the ring forms is roughly equal to the mass of the equilibrium ring. Using the instability condition expressed in equation (1), we may estimate the mass required for instability. As this involves an assumption of spherical shape, the resultant mass will only be approximately correct. We find that the mass limit M_* for instability is

$$M_* = 5.21 \times 10^{-23}\left[\frac{(R_g T/\mu + E_R)^3}{\rho}\right]^{1/2} M_\odot , \quad (4)$$

where the symbols are as defined earlier in the paper. Using the density ($\sim 10^{-16}$ g cm^{-3}), temperature (10 K), and E_R value which pertain to case 1D, we find $M_* = 0.25\ M_\odot$, in good agreement with the mass ($\sim 0.22\ M_\odot$) of the equilibrium ring for this case. The critical mass M_* is roughly proportional to $\rho^{-1/2}$, suggesting that if a gravitational instability is the cause of ring formation one would expect M_* for case 1B ($\rho = 3 \times 10^{-16}$ g cm^{-3}) and case 1A ($\rho = 2 \times 10^{-14}$ g cm^{-3}) to be $0.14\ M_\odot$ and $0.02\ M_\odot$, respectively. The values of T at the time of ring formation are identical in these cases, and the values of E_R are similar, so that the $M_* \propto \rho^{-1/2}$ scaling should be reasonably valid. The masses of the equilibrium ring in these two cases are $\sim 0.1\ M_\odot$ and $0.03\ M_\odot$, respectively, again in good agreement with the critical mass for instability. Although much more detailed work needs to be done on the question of ring formation, our results are consistent with formation as a result of a gravitational instability.

b) Ring Equilibrium

Ostriker (1964) has analytically calculated integral properties and structural characteristics of equilibrium, isothermal, self-gravitating rings whose thickness is small compared with the distance d of the ring from the rotation axis. He finds that equilibrium is only possible if the mass per unit length of the ring has the value $(M/L)_e = 2R_g T/(\mu G)$. The rings which form in cases 1B, 1C, 1D, 2A, and 5A are isothermal; however, the properties of the gravitational field in the ring formation region differ somewhat from those employed by Ostriker as a consequence of the presence of a flattened distribution of matter external to the ring.

As noted previously, the ring in case 1D was investigated in detail and found to be close to hydrostatic equilibrium. The calculated M/L value of this ring is 1.2×10^{16} g cm^{-1} compared with Ostriker's equilibrium value of $(M/L)_e = 1.24 \times 10^{16}$ g cm^{-1}. The estimated uncertainty in the numerical M/L ratios is 50 percent. The M/L values derived from Table 2 for cases 1B, 1C, and 2A are larger than the equilibrium values. An examination of the detailed force balance for these cases shows that they were beyond the equilibrium phase when the mass was calculated. The total angular momenta of the rings are within ~ 25 percent of the analytical values from Ostriker's study. The estimated uncertainty in the numerical J-values is 65 percent.

In addition to the integral characteristics, Ostriker's analysis yields the detailed structure (i.e., density profile) of an isothermal ring. He shows that the characteristic minor radius of the ring Δr, within which one-half of the ring mass is contained, is uniquely determined by the mass per unit length of the ring and the peak density ρ_0 in the ring. Ostriker's expression applied to case 1D yields $\Delta r = 1.5 \times 10^{15}$ cm. The value of Δr determined from the density contours of case 1D is 2.14×10^{15} cm in the R-direction and 1.0×10^{15} cm in the Z-direction, giving an average $\Delta r \approx 1.5 \times 10^{15}$ cm. The ellipsoidal cross-section of the numerical ring as contrasted to the circular cross section of the analytic ring is consistent with the difference in gravitational fields between Ostriker's case and ours. In summary, the integral properties and detailed structure of the equilibrium rings formed during the collapse are in good agreement with those of the analytic rings calculated by Ostriker.

An important question concerning these equilibrium rings is whether they are stable against nonaxisymmetric perturbations (NAPS). Using the numerically

determined internal and rotational energies of the rings in cases 1B, 1C, 1D, 2A, and 5A, and the virial theorem, we find the average β value for these rings to be 0.25 ± 0.05. The value of β obtained from application of Ostriker's formulae is approximately 0.24. This value is close to that (0.26 ± 0.02) at which the Maclaurin sequence and the sequence of differentially rotating polytropes become dynamically unstable to NAPS. There is, however, no evidence that suggests that rings will become unstable to NAPS at the same value of β as do the Maclaurin and polytropic sequences.

The existence of scaling laws between ring parameters and initial characteristics of the cloud would be most useful. Larson indicates that the ring radius d is roughly proportional to the cube of the initial angular velocity, ω_0, of the cloud. Our results are consistent with a scaling of that form between cases 1A and 1B. However, the d-value in Case 1B ($\beta = 0.08$) is approximately a factor of 2 smaller than the d-value in case 1C ($\beta = 0.32$), rather than the factor of 8 expected from the $\omega_0{}^3$ scaling. The scaling appears to break down when ω_0 is such that the initial model is close to centrifugal balance, as is case 1C. For a fixed value of β, however, the d-value of the rings scales approximately linearly with the mass of the cloud. As equilibrium rings are only possible for a specific value of the ratio $M/(2\pi d)$, this scaling implies that the fraction of the total cloud mass which is involved in the ring is independent of the total mass of the cloud (for fixed α, β). This fraction is ~ 10 percent for $\beta = 0.08$ and $\alpha = 0.52$. More work is needed to establish the generality and detailed nature of the scaling relations, with emphasis on a wider range of α- and β-values.

c) *Postequilibrium Ring Evolution*

Although the equilibrium phase just discussed is a quantitative characteristic of ring evolution, it is short lived. Ostriker's work shows that once the M/L value of the ring exceeds the critical value, equilibrium is no longer possible and the ring must collapse upon itself. This behavior is in fact observed. The gravitational field gradients steepen markedly inside the ring, concentrating most of the ring mass and a great deal of angular momentum into a small number of zones. This process occurs on a time scale comparable with the free-fall time of the ring.

Within a few free-fall times after the collapse of the ring has begun, the phenomenon of "sheet" ejection, discussed in § III*a* occurs. Any realistic discussion of the postequilibrium ring evolution must consider two problems: (1) at what value of β does an equilibrium ring become unstable to NAPS, and (2) is the phenomenon of sheet ejection real or is it a numerical artifact of the calculation?

Let us suppose that sheet ejection is numerical in origin. If future stability analyses of equilibrium, isothermal rings show that they are unstable to NAPS at $\beta = 0.25 \pm 0.05$, the rings would be expected to fragment along their length. Stability analysis may show that a higher β-value is required. However, as the rings collapse, β increases, and fragmentation could still occur, although an equilibrium stability analysis would no longer apply. Thus the likely postequilibrium ring evolution, in the event that sheet ejection is a numerical effect, is fragmentation into two or more distinct condensations, a suggestion that has been made by Larson (1972).

If the phenomenon of sheet ejection is real, fragmentation is not the inevitable fate of the ring. Several evolutions are possible. Even if the rings are dynamically unstable to NAPS at $\beta = 0.25 \pm 0.05$, the instability will manifest itself on a free-fall time scale, the same time scale as sheet ejection. In this case, sheet ejection and fragmentation could be concurrent phenomena. If the β-value for instability against NAPS is higher than the β-value for equilibrium rings, the evolution could be quite complex. As noted earlier, the β-value of the ring will increase as the ring collapses upon itself. However, once sheet ejection has occurred, it removes a great deal of the rotational energy of the ring. This "relief valve" effect may prevent the ring from ever reaching the critical β-value at which fragmentation occurs. Those rings whose evolution was followed beyond sheet ejection moved inward—that is, sheet ejection moves angular momentum out of the central regions of the cloud and moves mass inward. These possible evolutions are only meant to serve as indicators of the complexity of this phase of evolution. The exact nature of the evolution is an open question, probably requiring three-dimensional hydrodynamic calculations for its resolution.

d) *Further Questions Concerning the Evolution of the Cloud*

An alternative to the formation of a binary or multiple star system is of course the formation of a rotating nebula out of which planets and a single star might form. The most detailed model of such a hypothetical nebula is that of Cameron and Pine, which follows earlier work by Cameron (1969). These authors assume that the nebula was initially a uniformly rotating cloud with $\omega_0 \approx 7 \times 10^{-14}$ rad s^{-1} and radius $\sim 10^{17}$ cm. They do not calculate the dynamic collapse from this initial model, but simply assume that the initial rotating sphere flattens to a thin disk while preserving the angular momentum distribution of the original sphere (cf. Mestel 1963). Our case 2B is nearly identical to the initial model postulated by Cameron and Pine. As we have not followed the collapse to the point where all of the mass in the cloud has come into equilibrium, we cannot specify the final state in any detail. However, our results do show that the final equilibrium configuration (if one exists) will not be that calculated by Cameron and Pine. For example, the adiabatic ρ-T relation obtained in the center of the cloud as a result of our calculation is quite different from the one that they assume. In addition, there is a problem associated with obtaining a central condensation (the star) in the nebula. The time scale for the instabilities that occur

in the cloud is likely to be shorter than the time scale for transport of angular momentum outward. Unless the instabilities themselves result in transport of angular momentum (an interesting possibility) the inner portions of the cloud may well break up before the central condensation has a chance to occur. One might think that the problem could be resolved if the initial cloud had very low angular momentum so that rotational effects would not stop the collapse until the inner portions had reached stellar dimensions. However, an elementary calculation shows that the equilibrium radius of the nebular material outside the central object would be far too small to account for the orbits of the outer planets in the solar system. That is, if one assumes an initially uniformly rotating cloud, an angular momentum low enough to permit formation of the Sun would be too low to account for the outer planets. Thus, in order to understand the formation of the solar system, it seems necessary to appeal to either (1) an efficient mechanism which removes angular momentum from the central parts of the cloud before instabilities occur, or (2) a set of initial conditions—in particular, a distribution of angular momentum—quite different from that studied here.

e) Some Remarks on Axial Symmetry

One of the fundamental assumptions employed in the calculations discussed here is that the collapse is axisymmetric. It is reasonable to inquire whether this assumption is responsible, at least in part, for the ring structures found here, and whether this assumption is likely to be valid.

Lynden-Bell (1964) has pointed out that collapsing systems are only likely to maintain axial symmetry if pressure is important throughout much of the collapse and if density increases markedly toward the center. Both of these conditions obtain in the collapses studied here. More recent work (Stewart 1975) has shown that differentially rotating, equilibrium configurations may be unstable to NAPS, and that the instability leads to highly turbulent flow. As can be seen in Figure 1*c*, differential rotation is well established in case 1A after a time of 5×10^4 years; similar behavior occurs in the other cases studied here. One effect of the turbulence is to transfer angular momentum from the interior to the exterior regions of the cloud. Could this transfer mechanism, which is not included in the equations governing the dynamics, remove sufficient angular momentum from the ring-forming regions of the cloud to prevent ring formation, and give rise instead to a central condensation? A typical time scale for significant transport of angular momentum by turbulent viscosity is $\tau \approx L^2/\nu_{\rm turb}$, where L is the scale size of the system and $\nu_{\rm turb}$ is the kinematic viscosity due to turbulence, given roughly by $\nu_{\rm turb} \approx c_s l/3$ (c_s and l are, respectively, sound speed and mixing length). Therefore $\tau \approx 3L^2/c_s l$, or as $L \geq l$, $\tau \geq 3L/c_s$. Characteristic values of these parameters for case 1A yield $\tau \gtrsim 1.5 \times 10^5$ years, and a more realistic estimate of l would increase τ by at least a factor of 2. This time is significantly longer than the total evolution time to ring formation. Thus, although turbulent transport of angular momentum may be important in certain contexts, it does not seem fast enough to have significant influence on ring formation during the collapses studied here. Furthermore, unlike the configurations which were studied by Stewart, the differentially rotating configurations generated by collapse are not in equilibrium.

Although the arguments given above must be considered tentative, they indicate that ring formation is likely to proceed even if the assumption of axial symmetry is relaxed. Known nonaxisymmetric instabilities do not appear to operate on a sufficiently short time scale to have significant effects on the collapse dynamics up to the time of ring formation. However, once the ring has approached equilibrium, it is likely that it is subject to nonaxisymmetric breakup as suggested by Wong's recent (1974) stability analysis of equilibrium toroids.

f) Summary

The results of numerical hydrodynamic calculations show that the collapse of a rotating, axisymmetric cloud which conserves angular momentum leads to the formation of a ring structure in the interior of the cloud, confirming the result of Larson (1972) for clouds of 1 $M_\odot$. The general result holds true also for masses of 2 and 5 $M_\odot$, and for a considerable range of values of angular momentum. For a fixed value of β, if one considers the rings at the point of closest approach to equilibrium, the ring distance d is roughly proportional to the total mass, and the ratio of ring mass to total mass is independent of total mass (the value is about 10% for $\beta = 0.08$). For fixed mass and decreasing values of angular momentum J (or, equivalently, decreasing β at fixed α), rotational effects are delayed until higher values of central density are reached; the mass fraction contained in the ring and the ring distance decrease. If J is reduced far enough, the central regions become optically thick before ring formation occurs, but the general result is not affected. The properties of the ring are unaffected by a change in surface boundary condition from one of constant pressure to one of constant volume. The foregoing conclusions apply to calculations in which the initial density is assumed to be uniform throughout the cloud. However, if the initial density is assumed to decrease linearly with distance from the center, ring formation still takes place. More comprehensive studies of the effects of initial conditions have yet to be made. A calculation using the parameters and initial conditions appropriate for the Cameron-Pine model solar nebula gives results for the density distribution (ringlike) and the temperature-density relation in the inner regions which are not in agreement with that model. Furthermore, the occurrence of nonaxisymmetric instabilities may cause the cloud to break up and (speculatively) form a binary or multiple star system long before such an equilibrium is reached. Three-dimensional hydrodynamic calculations and a stability analysis of equilibrium rings should result in further progress regarding

quantitative treatment of mechanisms for angular momentum transport, such studies are necessary for an understanding of the conditions under which binary systems, on the one hand, or planetary systems, on the other, are formed.

We wish to thank Dr. J. LeBlanc for numerous discussions concerning numerical techniques. Professors L. Mestel, D. Lynden-Bell, and A. G. W. Cameron provided useful comments on questions of stability. Mr. J. S. Kennedy provided valuable assistance in the preparation of contour and velocity plots. We also thank Dr. D. McNally for his critical comments on the manuscript. We wish to acknowledge the kind hospitality of the University of London Observatory during the preparation of the manuscript. Detailed numerical data for the models presented here are available upon request from the authors. Partial funding for support of this study has been allocated by NASA-Ames Research Center under interchange NCAR 660-407 with San Francisco State University.

REFERENCES

Bardeen, J. M. 1971, *Ap. J.*, **167**, 425.
Black, D. C., and Bodenheimer, P. 1975, *Ap. J.*, **199**, 619 (Paper I).
Cameron, A. G. W. 1969, in *Low Luminosity Stars*, ed. S. Kumar (New York: Gordon & Breach).
Cameron, A. G. W., and Pine, M. R. 1973, *Icarus*, **18**, 377.
Goldreich, P., and Schubert, G. 1967, *Ap. J.*, **150**, 571.
Hara, T., Matsuda, T., and Nakazawa, K. 1973, *Progr. Theoret. Phys.*, **49**, 460.
Kippenhahn, R. 1969, *Astr. and Ap.*, **2**, 309.
Larson, R. B. 1972, *M.N.R.A.S.*, **156**, 437.
LeBlanc, J. M., and Wilson, J. R. 1970, *Ap. J.*, **161**, 541.
Lin, C. C., Mestel, L., and Shu, F. H. 1965, *Ap. J.*, **142**, 1431.
Lynden-Bell, D. 1964, *Ap. J.*, **139**, 1195.
Mestel, L. 1963, *M.N.R.A.S.*, **126**, 553.
Ostriker, J. P. 1964, *Ap. J.*, **140**, 1067.
Ostriker, J. P., and Bodenheimer, P. 1973, *Ap. J.*, **180**, 171.
Peaceman, D. W., and Rachford, H. H. 1955, *J. Soc. Indust. Appl. Math.*, **3**, 28.
Stewart, J. M. 1975, *Astr. and Ap.*, **42**, 95.
Tscharnuter, W. 1975, *Astr. and Ap.*, **39**, 207.
Wong, C. Y. 1974, *Ap. J.*, **190**, 675.

DAVID C. BLACK: Theoretical Studies Branch, Space Science Division, NASA-Ames Research Center, Moffett Field, CA 94035

PETER BODENHEIMER: Lick Observatory, University of California, Santa Cruz, CA 95064